Optical multicarrier generator for radio-over-fiber systems

Y. Kim, S. Doucet, M. E. Mousa Pasandi, and S. LaRochelle

Centre d'optique, photonique et laser (COPL), Department of Electrical and Computer Engineering, Université Laval, Québec, Canada, G1V 0A6
larochel@gel.ulaval.ca

Abstract: We propose an optical multicarrier generation method for radio-over-fiber (ROF) systems. The multicarrier generator is composed of a phase-modulated laser and two chirped fiber Bragg gratings used as flattening filters. The chirped gratings are spectrally tailored to equalize the intrinsically uneven envelope of the phase-modulated laser spectrum. A flattened multicarrier spectrum with 7 carriers at a frequency spacing of 12.5 GHz is demonstrated with less than 2 dB peak-to-peak variations and 40 dB optical signal-to-noise ratio (OSNR). We evaluate the quality of the multicarrier generator by using it as an externally modulated source for 802.11 compliant signals. We performed error vector magnitude (EVM) measurements on each of the filtered carrier and found an average value of -32.8 dB compared to -36.2 dB for a tunable laser source. The results show that the multicarrier source could be used for error free transmission.

OCIS codes: (060.2380) Fiber optics source and detectors; (060.5060) Phase modulation

References and links

1. K. Mori, H. Takara, and S. Kawanishi, "Analysis and design of supercontinuum generation in a single-mode optical fiber," J. Opt. Soc. Am. B **18**, 1780-1792 (2001).
2. J. Veselka and S. Korotky, "A multiwavelength source having precise channel spacing for WDM systems," IEEE Photon. Technol. Lett. **10**, 958-960 (1998).
3. M. Fujiwara, M. Teshima, J. –I. Kani, H. Suzuki, N. Takachio, and K. Iwatsuki, "Optical carrier supply module using flatteded optical multicarrier generation based on sinusoidal amplitude and phase hybrid modulation," J. Lightwave Technol. **21**, 2705-2714 (2003).
4. S. Bennet, B. Cai, E. Burr, O. Gough, and A. J. Seeds, "1.8-THz bandwidth, zero-frequency error, tunable optical comb generator for DWDM applications," IEEE Photon. Technol. Lett. **11**, 551-553 (1999).
5. Y. Kim, S. Doucet, and S. LaRochelle, "Multicarrier generator using a phase modulated laser signal and tailored chirped fiber Bragg gratings," in *Bragg Grating Photosensitivity and Poling* (Optical Society of America, Quebec, Quebec, 2007), paper BTuB4.
6. H. Kim, J. H. Cho, S. Kim, K. -U. Song, H. Lee, J. Lee, B. Kim, Y. Oh,, J. Lee, and S. Hwang, "Radio-over-fiber systems for TDD-based OFDMA wireless communication systems," J. Lightwave Technol. **25**, 3419-3427 (2007).
7. M. M. Sisto, M. E. Mousa Pasandi, S. Doucet, S. LaRochelle, and L. A. Rusch, "Optical phase and amplitude control for beamforming with multiwavelength Gires-Tournois Bragg grating cavities," in the P*roceedings of the Fourth IASTED Internationl Conference on Antennas, Radar and Wave* (International Association of Science and Technology for Development, Montreal, Quebec, 2007), pp. 238-243.
8. M. M. Sisto, S. LaRochelle, and L. A. Rusch, "Gain optimization by modulator bias control in radio-over-fiber links," J. Lightwave Technol. **18**, 1840-1842 (2006).
9. J. L. Corral, J. Marti, J. M. Fuster, and R. I. Laming, "True time-delay scheme for feeding optically controlled phased-array antennas using chirped-fiber gratings," IEEE Photon. Technol. Lett. **11**, 1529-1531 (1997).
10. Y. Liu, J. Yang, and J. Yao, "Continuous true-time-delay beamforming for phased array antenna using a tunable chirped fiber grating delay line," IEEE Photon. Technol. Lett. **14**, 1172-1174 (2002).
11. T. Sakamoto, T. Kawanishi, and M. Izutsu, "Asymptotic formalism for ultraflat optical frequency comb generator using a Mach-Zehnder modulator," Opt. Lett. **32**, 1515-1517 (2007).
12. M. Rochette, M. Guy, S. LaRochelle, J. Lauzon, and F. Trépanier "Gain equalization of EDFA's with Bragg gratings," IEEE Photon. Technol. Lett. **11**, 536-538 (1999)

#89690 - $15.00 USD Received 12 Nov 2007; revised 21 Dec 2007; accepted 3 Jan 2008; published 14 Jan 2008

1. Introduction

Multicarrier optical sources with narrow channel spacing have emerged to meet demands from networks with dense wavelength-division-multiplexing and superdense WDM. Many solutions have been proposed to achieve low-cost compact multicarrier optical sources that would provide all the channels required by optical communication standards. These schemes are based on supercontinuum (SC) generation [1], nonlinear spectral broadening of intensity modulated signals [2], hybrid modulation with $LiNbO_3$ modulators [3], and phase modulation in regenerative erbium-doped fiber amplifier loop [4]. Recently, for the purpose of ROF applications, we proposed a simple and efficient multicarrier generation source based on the equalization of a phase-modulated spectrum by carefully tailored chirped fiber Bragg gratings [5].

Nowadays ROF networks attract much attention because they provide an end-to-end and cost-effective solution for inherent problems of the wireless channel, such as loss, complexity and bandwidth limitation. The combination of the wireless and optical channels for implementing the multiple-inputs multiple-outputs (MIMO) concept recently raised much research interest because of the challenges in transmitting analog modulation formats and in feeding multiple antenna systems [6]. Wavelength multiplexing can be used advantageously to accomplish RF null-steering beamforming by externally modulating a multicarrier optical source by the analog signal and processing the optical signal with the null-steering beamformer with multiple wavelength capabilities [7]. The signal is then transmitted over the optical fiber followed by optical carrier demultiplexing and photodetection at the antenna site. This modulation and beamforming strategy enables us to not only reduce the number of required laser source but also to take advantage of external modulator bias optimization [8] in order to increase RF gain and avoid the use of RF amplifiers chain for each channel as recently reported for implementing MIMO [6]. As a single optical carrier is assigned to each antenna element, multiple optical carriers with good noise properties are essential to deliver radio frequency signals to phased-array antennas. Currently, most of the reported ROF systems rely on multiple externally-modulated distributed-feedback semiconductor lasers as multicarrier transmitter [9, 10]. This approach does not provide a cost-effective and wavelength scalable solution.

In this paper, we present a novel multicarrier generator optical source for ROF applications. This simple method produces a flattened multicarrier spectrum by combining a phase modulated laser signal with apodized chirped fiber Bragg gratings (CFBGs) that are carefully tailored to equalize the optical carrier power. The CFBGS are transmission gratings with an apodized index profile designed with an iterative algorithm. After the equalizing filters, less than 2 dB peak-to-peak deviations is found among 7 optical carriers spaced by 12.5 GHz and the optical signal-to-noise ratio (OSNR) is better than 40 dB. To characterize the performance of this novel multicarrier generator, we examined the transmission quality of IEEE 802.11a signal, which is based on orthogonal frequency division multiplexed (OFDM) technique and 64-QAM modulation format. In order to verify the microwave signal quality carried by each optical frequency, error vector magnitude (EVM) measurements were performed for all filtered optical carriers. The results are compared to the measurement made on the externally modulated signal of an external cavity laser diode with high spectral purity. Considering that the dense constellation and close spacing of IEEE 802.11a OFDM subcarriers makes sensitive to noise and distortion, this measurement demonstrates the capability of this laser source not only for this format but also for other existing ROF signal transmission.

2. Experiments and discussion

2-1. Flattened optical multicarrier generator

For telecommunication applications, multicarrier generation techniques using $LiNbO_3$ modulator have superior features when compared to other suggested methods. The phase modulators generate several sidebands that have the same characteristics as the incident

#89690 - $15.00 USD Received 12 Nov 2007; revised 21 Dec 2007; accepted 3 Jan 2008; published 14 Jan 2008

continuous wave (CW) laser signal in terms of polarization, relative intensity noise (RIN) and phase noise. However, if the number of sidebands is increased by using a higher modulation index, their power rapidly becomes uneven. This behavior is intrinsic to the well-known response of a phase-modulated signal with a sinusoidal driving voltage for which the amplitude of each sideband is related to the Bessel function of the first kind. To overcome this difficulty, it was proposed to use a hybrid modulation scheme that combines a Mach-Zehnder amplitude modulator and a phase modulator [3]. This tandem modulation method provided a flat multicarrier spectrum with peak-to-peak variations less than 2 dB over 9 generated frequencies and with an optical signal to noise ratio (OSNR) of 33 dB. However, this technique requires strict synchronization of the respective RF signals applied to the two modulators and therefore needs a large number of electrical and electro-optical components including the two modulators with RF amplifiers, multiple electrical devices and RF phase shifter. Recently another method was theoretically suggested using a Mach-Zehnder $LiNbO_3$ modulator to obtain an ultra-flattened multicarrier spectrum but it requires a dual-drive Mach-Zehnder modulator and two very high power (9 Watts for each) RF signals for both arms of the modulator in order to achieve a high modulation index (~6π) [11].

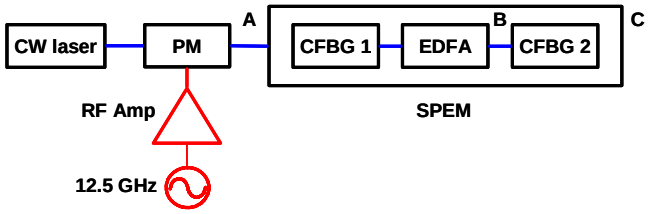

Fig. 1. Schematic diagram of the proposed multicarrier generator composed of a CW laser, a phase modulator (PM), and a sideband power-equalizing module (SPEM) with an EDFA sandwiched between the two tailored CFBGs

A more direct and intuitive way to generate a flattened multicarrier spectrum via a phase modulator (PM) is to introduce a matched loss profile to the phase-modulated spectrum. As the amplitudes of the sidebands are solely dependent on the modulation index at a given modulation frequency, the specific loss profile needed to flatten the phase-modulated spectrum can be easily calculated. The experimental configuration of the proposed flattened multicarrier generator is presented in Fig. 1. It is composed of three parts: a continuous wave (CW) laser (a DFB laser diode), a PM, and a sideband power equalizing module (SPEM). In the SPEM, we inserted an erbium-doped fiber amplifier (EDFA with 25 dB gain) between two spectrally tailored CFBGs to compensate insertion loss of the first CFBG and to simultaneously increase the optical power of the generated sidebands. The maximum RF power available from the RF amplifier was 24 dBm and, with this value, the maximum modulation index of the PM was 0.86π. The SPEM configuration allows wavelength scalability which can be easily achieved by increasing the number of seeded carriers to a PM and increasing the bandwidth of the flattening optical filters. This is possible because $LiNbO_3$ shows a uniform electro-optic response over a large optical band and because the loss profile covering the multicarriers generated from several seed lasers could be obtained cascading filters designed by simply shifting the center wavelength of the initial grating design.

To start with a spectrum that would be as flat as possible, we adjusted the modulation index of the phase modulator to the value that yields the smoothest envelope for the -3 to +3 sidebands. The corresponding modulation index was 0.68π and the phase-modulated laser spectrum measured before the SPEM (point A in Fig. 1) is shown in Fig. 2(a). In this phase-modulated laser spectrum with 12.5 GHz spacing we find that the maximum peak-to-peak power variation among the 7 central sidebands is around 12 dB. As was previously discussed, the steep envelope is a result of the phase-modulation process. The 12 dB power variation combined to the dense 12.5 GHz spacing of these carriers poses great challenges to the CFBG flattening filters. Previous work on flattening filters has mostly been done in the context of gain equalization of erbium doped fiber amplifiers [12]. In this case, the requirements in terms

#89690 - $15.00 USD Received 12 Nov 2007; revised 21 Dec 2007; accepted 3 Jan 2008; published 14 Jan 2008

of spectral loss variations are less stringent and chirped phase masks covering the whole C-band can be used to achieve the desired spectral response. In the present case, even with a 0.5 nm/cm chirp phase mask, it was impossible to achieve the steep loss variations with a single CFBG and we had to rely on a cascade of two CFBGs. The transmission spectra of the first CFBG (CFBG 1), the second CFBFG (CFBG 2), and the SPEM (CFBG 1+CFBG 2) are presented in Fig. 2(b), along with the flattened multicarrier spectrum measured after the SPEM (point C in Fig. 1) that is presented in Fig. 2(c). The falttened spectrum has less than 2 dB peak-to-peak power variations among the seven optical carriers spaced by 12.5 GHz. In the following paragraph, we detail the design and fabrication of the CFBGs. All the optical spectra shown in the paper were measured with an OSA with a 0.01 nm resolution bandwidth.

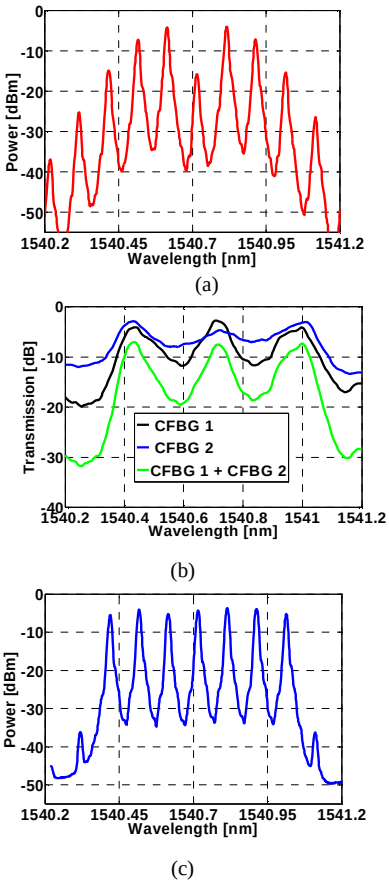

Fig. 2. (a). Phase-modulated optical spectrum before the SPEM (point A), (b) transmission loss spectrum of the SPEM filters, and (c) flattened multicarrier spectrum after the SPEM (point C).

2-2. Design and fabrication of the spectrally tailored CFBGs

In addition to flatten the phase-modulated spectrum, another important function of the CFBG filters is to suppress the unnecessary sidebands. This desirable to allow multiplexing of wavelength bands carrying different ROF signals feeding different antenna arrays. Suppression of the higher order sidebands is therefore required to avoid crosstalk between these ROF signals. To perform the design of the bandpass flattening filters, we had to develop an iterative algorithm. Indeed, taking into account the fact that the grating design is constrained by the available linearly chirped phase masks, it is not possible to use standard inverse scattering algorithms because they would inevitably lead to gratings with nonlinear chirp, even if the initial target is the reflection spectrum calculated from the desired

#89690 - $15.00 USD Received 12 Nov 2007; revised 21 Dec 2007; accepted 3 Jan 2008; published 14 Jan 2008

transmission spectra and from the linear reflection group delay related to the phase mask chirp. Furthermore, Fourier transform and traditional CFBG relationships between apodization profiles and reflection spectra are not applicable to the design of the flattening filters because of the high reflectivity and dense amplitude variations. Finally, the design must also consider the UV beam width that limits the feature size of the apodization profile.

The iterative algorithm that determines the required apodization profile of each CFBG is described in Fig. 3. We first specify the filter stop band with the proper spectral width and extinction ratio to ensure sufficient suppression of the undesired sidebands. We then construct the target spectrum T_{TAR} for the CFBG filter by combining the stop band spectrum with the loss profile required to flatten the experimentally measured phase-modulated spectrum.

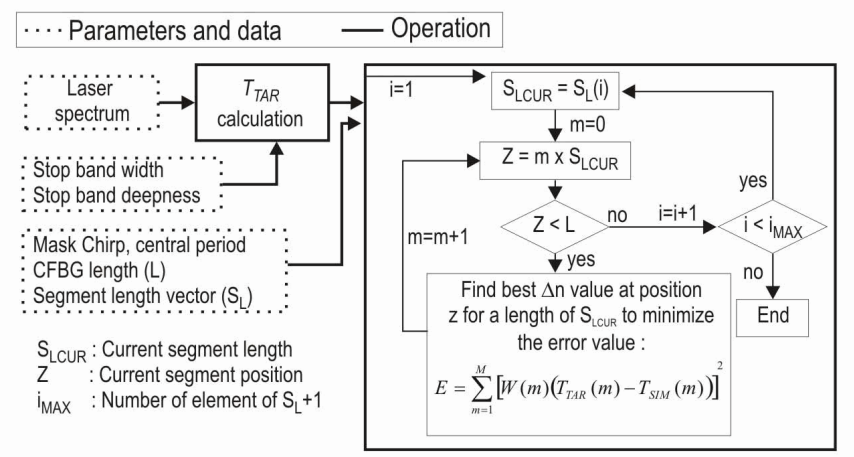

Fig. 3. Details of the iterative algorithm for the tailored chirped Bragg grating design.

Other parameters such as the phase mask chirp rate, the central period and the length of the CFBG are also specified before running the iterative algorithm. With all these parameters, the algorithm finds the apodization profile that minimizes for each iteration step the error value (E) calculated from T_{TAR} and the simulated spectrum (T_{SIM}). This error value is calculated by using a vector (W) that introduces different weights to the error between T_{TAR} and T_{SIM} for all the spectral samples. In our calculations, the error is weighted by a factor of two for the spectral region which includes the desired output laser lines and a unitary factor for the others spectral samples. The grating spectral response is calculated using a vector containing different step lengths S_L defined as the grating length over which the UV induced refractive index change, Δn, is assumed to be uniform. The values of Δn are selected to minimize the weighted differences at actual segment positions z. To ensure the gradual convergence towards the target spectrum, the segment length is set to be the longest at the beginning of the process and is steadily reduced up to a minimum length of the order of the minimum UV beam width that is approximately 250 μm in our writing setup. The design was done by considering a phase mask chirp of 0.5 nm/cm. The target transmission spectra T_{TAR} and the simulated spectra of the two designed gratings T_{SIM} are compared in Fig. 4. Even though we found that an optimum grating design for the first CFBG should flatten the phase-modulated spectrum with less than 2 dB peak-to-peak variations as shown in Fig. 4(c) and more clearly in the inset, we experimentally achieved only 6.1 dB flatness among 7 sidebands. We therefore proceeded to the design of a second CFBG (CFBG2) based on the measured spectrum after the EDFA. The discrepancy between the simulated and experimental results is caused by local writing errors, mostly in the spectral region between 1540.9 and 1541 nm in Fig. 4(c). We believe that the designed transmission dynamic range of more than 12 dB made the chirped grating spectral response very sensitive to apodization errors. Even with the best CFBG, power equalization would inherently be limited to 2 dB. We therefore decided to

#89690 - $15.00 USD Received 12 Nov 2007; revised 21 Dec 2007; accepted 3 Jan 2008; published 14 Jan 2008

design a second CFBG to correct the power variations that had already been reduced to 6.1 dB by the first grating and closer agreement was obtained between the experimental and the simulations results for this second grating. The apodization profiles for each CFBG are shown in Fig. 4(a) and Fig. 4(b) where it can be seen that we took advantage of the weighted error function of the iterative algorithm to obtain a better fit over the main region of interest [insets of Fig. 4(c) and Fig. 4(d)]. The largest deviations between T_{TAR} and T_{SIM} are observed in the filter stop band.

The gratings were fabricated in hydrogen loaded photosensitive cladding mode suppression fiber by using phase mask scanning. The apodization profile is made by phase mask dithering. Figure 4 shows the experimental results obtained for both CFBG filters. Figure 5 displays the optical spectra measured at three positions; at the SPEM input (point A), just after the EDFA (point B) and at the SPEM output (point C). Peak-to-peak power variations are reduced from 11.7 dB to 6.1 dB with the first CFBG filter and further decreased to less than 1.8 dB after the second one. At the SPEM output, we therefore obtain 7 optical carriers spaced by 12.5 GHz with less than 2 dB power variations and with an OSNR better than 40 dB and a sideband suppression ratio of more than 30 dB. The total output power of the multicarrier spectra is 6.4 dBm.

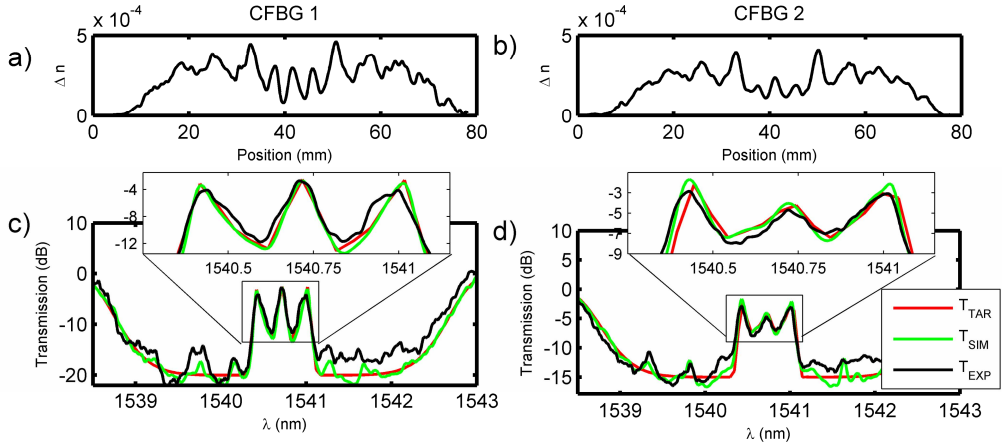

Fig. 4. Characteristics of the two CFBGs, (a) and (b) the apodization profile of the CFBG 1 and CFBG 2 respectively, (c) and (d) transmission spectra of CFBG 1 and CFBG 2 respectively plotted with the target transmission spectra T_{TAR}, the simulated spectra T_{SIM}, and the experimental result T_{EXP}.

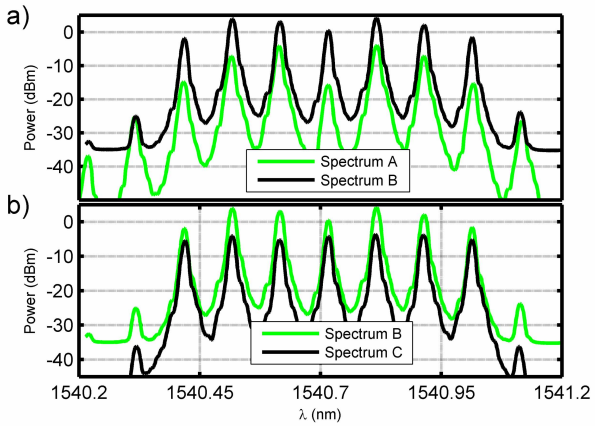

Fig. 5. Output spectra at different points of the multicarrier generation procedure; Spectrum A at the input of the SPEM, spectrum B after the first CFBG and an EDFA, and Spectrum C at the output of the SPEM

#89690 - $15.00 USD Received 12 Nov 2007; revised 21 Dec 2007; accepted 3 Jan 2008; published 14 Jan 2008

2-3. EVM measurement of the multicarrier generator

The multicarrier generator was tested in a transmission link to assess to quality of the generated carriers for transmission of ROF signals. The ROF link consisted of a multicarrier generator, an EDFA, a Mach-Zehnder modulator, a uniform FBG used a tunable filter to isolate one frequency band and an amplified photodetector. In the final application, the multicarrier signals should be able to carry IEEE 802.11 compliant signals to an optical null-steering beam former. After the beam former, they will be wavelength demultiplexed to be coupled to the various elements of an antenna array. Therefore, the quality of the modulated signal transmitted by each optical carrier must be high enough to lead to good ROF performance.

The IEEE 802.11a/g for wireless local area network (LAN) is based on OFDM modulation with 20 MHz bandwidth and RF carrier frequencies of 2.5 or 5 GHz. The 20 MHz bandwidth is divided to 52 subcarriers data tones that can be modulated by multi-level quadrature amplitude modulation (QAM). The 802.11a maximum transmission rate of 54 Mb/s is achieved using a dense 64-QAM constellation that is very sensitive to link noise and distortion. To verify the quality of the OFDM signal, EVM measurements were performed. The EVM parameter is given as

$$EVM_{dB} = 10\log_{10}\left(\frac{\sum_{n}|r_n - z_n|^2}{\sum_{n}|r_n|^2}\right), \quad (1)$$

where r represents the transmitted 64-QAM symbols and z is the received ones [8]. The EVM is equal to the ratio of the power of the error vector to the root mean square (RMS) power of the transmitted symbols without any errors. IEEE 802.11a protocol imposes -25 dB as the maximum allowable EVM value for error free transmission.

The complete experimental setup used for EVM measurement is schematically described in Fig. 6. The $LiNbO_3$ Mach-Zehnder modulator bias is set at the quadrature point (halfwave voltage) in order to increase modulation efficiency and reduce distortion [8]. The RF input to the modulator was provided by a vector signal generator (VSG). The tunable filter consisted of a circulator and a uniform FBG with a full-width at half-maximum bandwidth of 6.5 GHz. The grating was strained tuned to select the desired modulated carrier signal and the neighboring carriers were suppressed by more than 15 dB. The filtered signal was sent to an amplified photodetector and the received RF signal was fed to a vector signal analyzer (VSA) synchronized with the VSG. The electrical back-to-back EVM measurement, with the VSG directly connected to the VSA, was -48.7 dB.

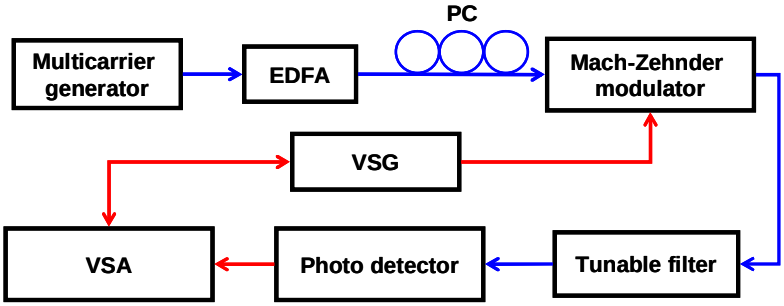

Fig. 6. Schematic diagram used for the EVM measurements of the proposed multicarrier generator

#89690 - $15.00 USD Received 12 Nov 2007; revised 21 Dec 2007; accepted 3 Jan 2008; published 14 Jan 2008

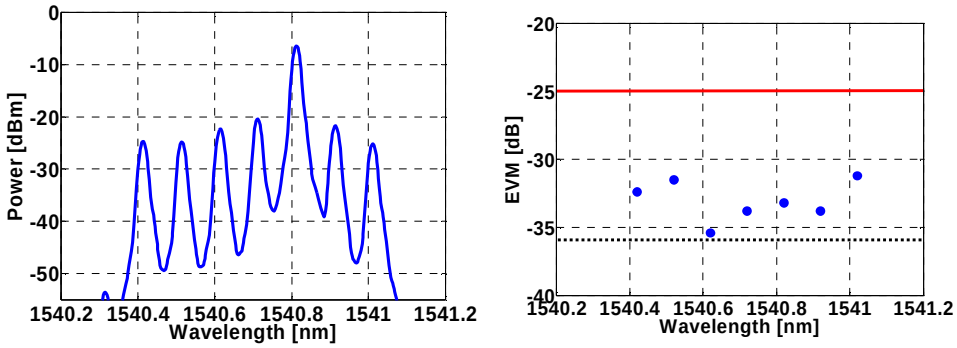

(a) (b)

Fig. 7. (a). Optical spectrum of the multicarrier signal measured after the tunable filter is set to the positive first order sideband (b). EVM values measured for all multicarriers.

Figure 7 shows an example of an optical spectrum measured after the single tunable filter tuned to an optical carrier located at 1540.82 nm. Other carriers were suppressed by 15 dB due to the sharp FBG transmission function. In this case the measured EVM value was -33.2 dB. When the other carriers were selected the measured EVM values were in the range of -31.2 dB to -35.4 dB, far better than the -25 dB standard threshold described in red trace in Fig. 7(b) that guarantees error free transmission. The average EVM value of all seven carriers shown in Fig. 7(b) was – 32.8 dB. To have a reference, we performed the EVM measurement by use of a tunable laser source as a carrier excluding the EDFA and the tunable optical filter in the EVM measurement setup. During the measurements the optical power of the tunable laser source was set at 5 dBm which corresponded to the optical input power of each carrier transmitting the Mach-Zehnder modulator. EVM measurement values did not show any noticeable wavelength dependence within the narrow spectral region (75 GHz span). The average EVM value measured was -36.2 dB and found in black dots in Fig. 7(b). The degradation from -48.7 dB to -36.2 dB in EVM arises from Mach-Zehnder third-order distortion [8]. Therefore degradations of EVM values in comparison with the result using a tunable laser source were induced by the non-perfectly flat envelope of the multicarrier and instabilities of fiber Bragg gratings (CFBGs and a tunable FBG) as no efforts were taken to stabilize them against any external perturbations at this experiment. Better EVM measurement results are surely expected by use of a lowered chirp rated phase mask than 0.5 nm/cm and implementing proper packaging's on FBGs. It is also worth of noting that during the experiment any adjustment of the polarization state of the sideband was unnecessary as optical multicarriers were obtained from the phase modulation of a laser signal and this is a most desirable necessity for ROF systems as all optical carriers is modulated by a single Mach-Zehnder modulator at the whole ROF systems.

3. Conclusion

In this paper, we proposed a method to generate multiple optical carriers from a phase-modulated laser signal. Two CFBGs passband filters were spectrally tailored using an iterative algorithm to flatten the power spectrum and to suppress the unwanted sidebands. A power uniformity better than 2 dB was obtained among 7 carriers despite the close frequency spacing (12.5 GHz) of the sidebands. Flattening of the optical power spectra could be achieved with a single CFBG if the carriers had a larger frequency spacing, for example 25 GHz, or if a lower phase mask chirp was used. In all cases, this would be achieved at the expense of the grating length, which could make packaging more challenging. With suppression of the unwanted sidebands by more than 30 dB and OSNR better than 40 dB, the quality of the proposed multicarrier generator was shown to be adequate for the distribution of 64-QAM IEEE 802.11a signals which are known to be sensitive to phase noise and distortion. The measured EVM value, -32.8 dB on average, is well below the standard threshold for error free

#89690 - $15.00 USD Received 12 Nov 2007; revised 21 Dec 2007; accepted 3 Jan 2008; published 14 Jan 2008

transmission. With this multicarrier generator, the number of carriers available from one seed laser is proportional to the modulation index of the PM. For an instance to obtain a larger number of carriers than in the current experiment, the modulation index needs to be increased to 1.42π (11 carriers) which would require 28 dBm of RF power considering the V_π value of our PM. The combination of a lower V_π PM and a high power RF amplifier should definitely support much higher modulation index and both devices are commercially available with relatively low cost nowadays. Further wavelength scalability of the proposed multicarrier generation is achievable by cascading tailored CFBGs with each spectral center wavelength corresponding to seeded carriers.

Acknowledgments

The authors are thankful to M. M. Sisto for the fruitful discussions on OFDM. Y. Kim acknowledges the financial support of the Fonds Québécois de la Recherche sur la Nature et des Technologies (FQRNT). This work was supported in part by the National Science and Engineering Research Council of Canada and by the Canada research chair in Optical fibre communications and components.

#89690 - $15.00 USD Received 12 Nov 2007; revised 21 Dec 2007; accepted 3 Jan 2008; published 14 Jan 2008